Neuron
Article

# Circuits for Grasping: Spinal dI3 Interneurons Mediate Cutaneous Control of Motor Behavior

Tuan V. Bui,[2] Turgay Akay,[3,4] Osama Loubani,[2] Thomas S. Hnasko,[5] Thomas M. Jessell,[3] and Robert M. Brownstone[1,2,*]
[1]Department of Surgery (Neurosurgery)
[2]Department of Medical Neuroscience
Dalhousie University, Halifax, Nova Scotia B3H 4R2, Canada
[3]Departments of Neuroscience and Biochemistry and Molecular Biophysics, Kavli Institute for Brain Science, Howard Hughes Medical Institute
[4]Department of Neurological Surgery, Center for Motor Neuron Biology and Disease
Columbia University, New York, NY 10032, USA
[5]Department of Neurosciences, University of California San Diego, La Jolla, CA 92093, USA
*Correspondence: rob.brownstone@dal.ca
http://dx.doi.org/10.1016/j.neuron.2013.02.007

## SUMMARY

**Accurate motor performance depends on the integration in spinal microcircuits of sensory feedback information. Hand grasp is a skilled motor behavior known to require cutaneous sensory feedback, but spinal microcircuits that process and relay this feedback to the motor system have not been defined. We sought to define classes of spinal interneurons involved in the cutaneous control of hand grasp in mice and to show that dI3 interneurons, a class of dorsal spinal interneurons marked by the expression of Isl1, convey input from low threshold cutaneous afferents to motoneurons. Mice in which the output of dI3 interneurons has been inactivated exhibit deficits in motor tasks that rely on cutaneous afferent input. Most strikingly, the ability to maintain grip strength in response to increasing load is lost following genetic silencing of dI3 interneuron output. Thus, spinal microcircuits that integrate cutaneous feedback crucial for paw grip rely on the intermediary role of dI3 interneurons.**

## INTRODUCTION

Coordinated movement relies on the integration of sensory feedback signals with core motor circuits. In mammals, motor performance is refined by sensory feedback signals that convey information from proprioceptive afferents as well as from mechanoreceptive afferents activated by diverse cutaneous receptors. This information is integrated in spinal motor circuits to ensure that intended movements conform to the environmental context. Defining spinal microcircuits involved in the integration of sensory inputs represents one approach to obtaining insight into the physiological control of motor actions.

Studies of sensory integration in spinal motor microcircuits have largely focused on the influence of proprioceptive inputs on spinal neurons in the cat (Jankowska, 2008; McCrea, 2001). In recent years, the use of molecular genetic techniques has yielded insight into the integration of proprioceptive afferent activity in motor circuits in mice (Mentis et al., 2006; Pecho-Vrieseling et al., 2009; Sürmeli et al., 2011; Tripodi et al., 2011;Wang et al., 2008). Cutaneous afferents also regulate the output of spinal motor circuits, most notably in the control of locomotion (Burke et al., 2001; Drew and Rossignol, 1987; Duysens and Pearson, 1976; Forssberg, 1979; Quevedo et al., 2005), but the identity and circuitry of spinal interneurons that process and transmit cutaneous afferent signals to motoneurons remain largely unknown.

Studies of interneurons comprising spinal circuits have typically relied on locomotor activity as the assay of motor circuit function (Brownstone and Bui, 2010; Fetcho and McLean, 2010; Grillner and Jessell, 2009). Many of the core features of locomotor activity can be produced by "central pattern generators"—for example, the fundamental rhythm and pattern of walking can be obtained without sensory feedback. In contrast, motor activities, such as object manipulation and hand grip, appear to be more dependent on cutaneous sensory input (Witney et al., 2004).

Emerging evidence indicates that sensory feedback from cutaneous mechanoreceptors regulates the force and precision of grasp tasks (Witney et al., 2004). Moreover, spinal interneurons active during grip have been recorded in the macaque monkey (Fetz et al., 2002; Takei and Seki, 2010), but it remains unclear whether the activity of these interneurons is influenced by sensory feedback and whether these neurons actually play a critical role in the spinal circuits for grip control. Short-latency cutaneous-evoked reflexes to motoneurons have been identified in the cat (Egger and Wall, 1971; Hongo et al., 1989a, 1989b; Moschovakis et al., 1992), supporting the existence of excitatory interneurons involved in the integration of cutaneous sensation. However, the involvement of such interneurons in motor behavior is not known.

In this study, we aimed to define and manipulate, through their distinguishing molecular character, sets of spinal interneurons with roles in mediating cutaneous control of motor output relevant to grasping. We reasoned that spinal interneurons that control grip would be located in deep dorsal and/or intermediate laminae, the site of termination of cutaneous afferents (Brown

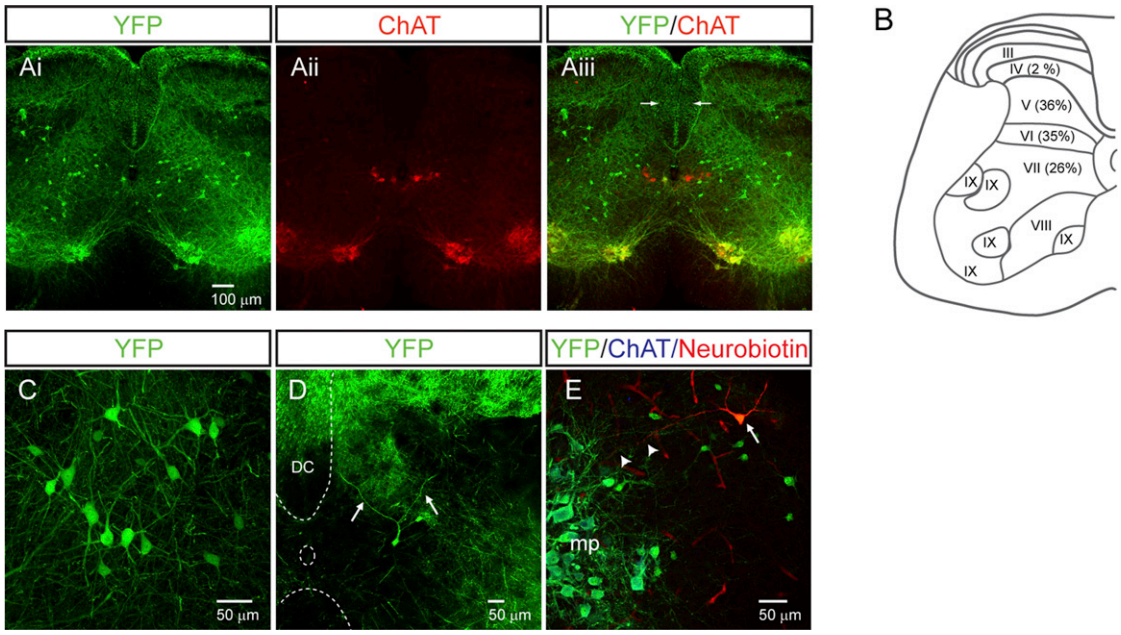


**Figure 1. dI3 INs Are Multipolar Spinal Interneurons Located in the Deep Dorsal Horn and the Intermediate Laminae of the Spinal Cord**

(A) Transverse distribution of YFP- and ChAT-labeled spinal neurons in a lumbar spinal cord section. Note the expected expression in dorsal root ganglion neurons, as seen by fluorescence in axons in the dorsal columns (arrows) and dorsal horns.

(B) Laminar distribution of dI3 INs based upon cell counts from ten transverse L4 and L5 sections. Laminae divisions are based upon those described in Watson et al. (2008).

(C) dI3 INs are multipolar neurons with multiple dendrites. The somata of dI3 INs were of intermediate size (17.5 ± 3.7 μm, n = 95) and multipolar in shape with, on average, 3.9 ± 3.7 (n = 95) primary dendritic trees.

(D) A dI3 IN with dendrites (arrows) extending into laminae IV–VI of the dorsal horn. Dorsal column (DC), central canal (oval), and ventral white matter are delineated by dashed curves.

(E) A neurobiotin-filled dI3 IN (arrow) with dendritic process (arrowheads) extended toward motor pools (mp).

All images are from *Isl1*-YFP mice. See also Figure S1.

et al., 1981; Todd, 2010). We focused on a class of neurons called dI3 interneurons (dI3 INs) (Ericson et al., 1992; Gross et al., 2002; Müller et al., 2002). dI3 INs represent one of six classes of "early-born" dorsally-derived interneurons and can be distinguished from other spinal interneurons by their expression of the LIM homeodomain transcription factor Isl1 (Helms and Johnson, 2003; Liem et al., 1997). We show that dI3 INs form excitatory glutamatergic synapses with motoneurons and, in turn, receive low-threshold cutaneous afferent input. Eliminating glutamatergic transmission from these interneurons results in a profound loss of grip strength. Therefore, dI3 INs are an interneuron class that is necessary for the spinal interneuronal microcircuits crucial for cutaneous regulation of paw grasp.

## RESULTS

### dI3 INs Are Located in Intermediate Laminae

The location of yellow fluorescent protein $(YFP)^+$ dI3 INs and choline acetyltransferase $(ChAT)^+$ motoneurons was determined in P13–P20 *Isl1*$^{+/Cre}$; *Thy1-lox-stop-lox-YFP* (*Isl1*-YFP) spinal cord. YFP$^+$/ChAT$^{null}$ dI3 INs (Figures 1Ai–1Aiii) were present along the length of the spinal cord and were detected in roughly equal proportions in laminae V, VI, and VII in the lumbar (Figures 1B–1E) and cervical (Figure S1 available online) spinal cord in regions where cutaneous afferents from the limbs are known to terminate (Todd, 2010).

### dI3 INs Are Glutamatergic Premotor Interneurons

We determined the transmitter phenotype of dI3 INs by assessing the expression of the vesicular glutamate transporter vGluT2 in Isl1-YFP$^+$ INs in P13–P20 mice. We found that ~85% of dI3 INs expressed vGluT2 (Figure 2A). The presence of vGluT2$^{null}$/YFP$^+$ autonomic motoneurons in rostral sections combined with the imperfect sensitivity of this technique may have led to an underestimate of the true proportion of glutamatergic dI3 INs. None of the Isl1-YFP$^+$ boutons expressed GlyT2, GAD65, or GAD67 (data not shown), indicating that dI3 INs are neither glycinergic nor GABAergic. Altogether, these data indicate that the vast majority of, and probably all, dI3 INs possess glutamatergic transmitter phenotypes.

We determined whether dI3 INs form direct connections with spinal motoneurons by examining spinal cords from *Isl1*$^{+/Cre}$; *Thy1-loxP-stop-loxP-mGFP* mice, in which Cre-directed, membrane-bound GFP labels a small proportion (<1%) of Isl1-expressing neurons and their axons. We detected GFP$^+$ axons, which formed bouton-like varicosities along motoneuron dendrites (Figure 2B). Furthermore, after intracellular injections in dI3 INs in *Isl1*-YFP mice, neurobiotin-labeled axons with

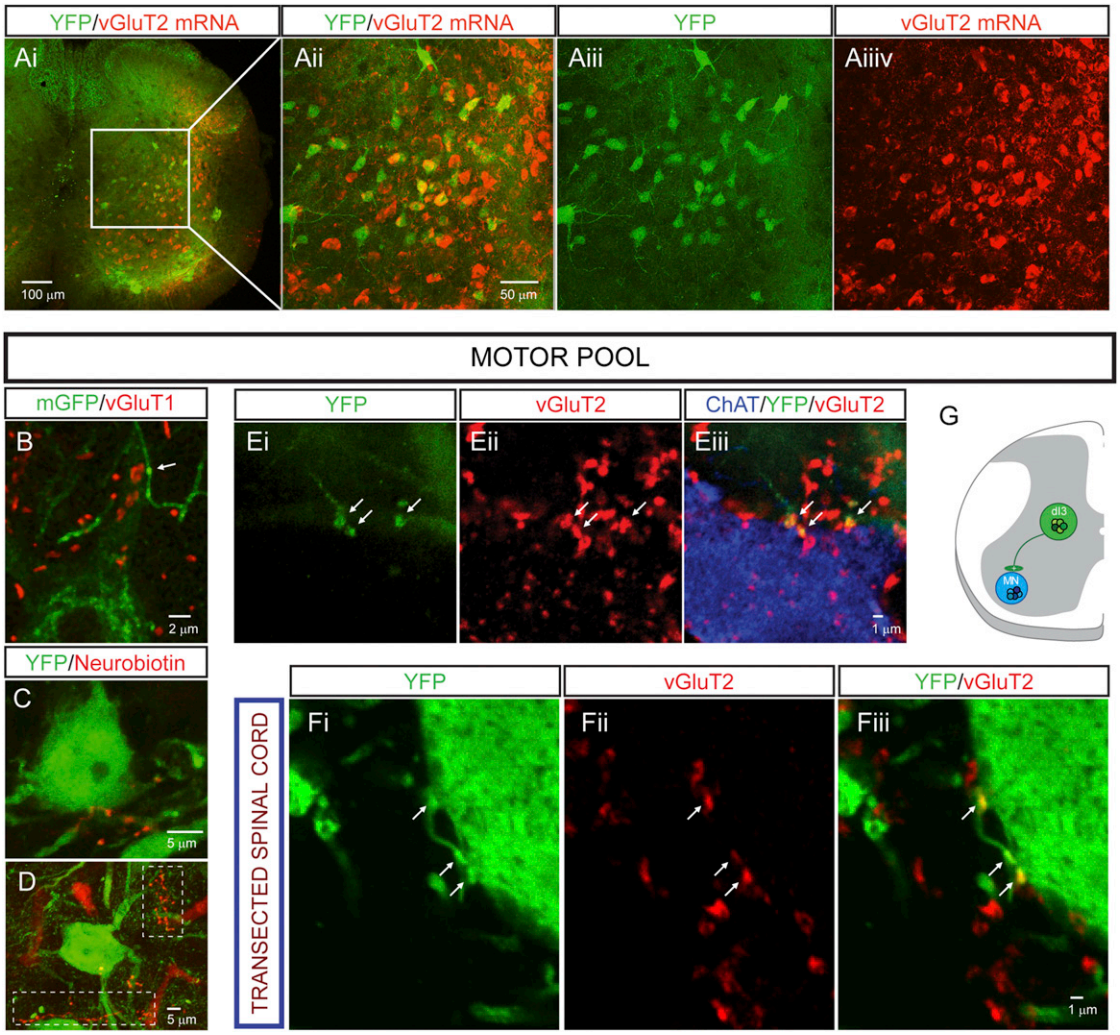


**Figure 2. dI3 INs Are Excitatory Premotor Interneurons**

(A) In situ hybridization for *vGluT2* mRNA colocalizes with YFP$^+$ interneurons in laminae V–VII. Quantitative analysis was restricted to laminae V–VII to avoid sampling YFP$^+$ somatic motoneurons in lamina IX and revealed that 118/139 YFP$^+$ neurons clearly expressed vGluT2.

(B) YFP$^+$ motoneuron in lamina IX with YFP$^+$ bouton-like structures (arrow) from putative dI3 INs in a spinal cord of an *Isl1*$^{+/Cre}$; *Thy1-lox-stop-lox-mGFP* mouse. vGluT1 is labeled in red, demonstrating that these processes are not from primary afferents.

(C and D) YFP$^+$ motoneurons in the lamina IX motor pool with bouton-like processes from neurobiotin-labeled dI3 IN. Thick red processes are blood vessels. White dashed boxes highlight clusters of filled boutons.

(E) vGluT2$^+$/YFP$^+$ boutons (arrows) in apposition with motoneuron (labeled with ChAT).

(F) vGluT2$^+$/ YFP$^+$ boutons (arrows) apposed onto motoneuron processes in chronically transected spinal cord.

(G) A diagram representing dI3 INs as last-order, excitatory interneurons.

Unless otherwise noted, all images are from *Isl1*-YFP mice. See also Figure S2.

bouton-like structures were detected in apposition to the dendrites of YFP$^+$ motoneurons (Figures 2C–2D), often seen as clusters of boutons (Figure 2D, dashed boxes). We also detected vGluT2$^+$/YFP$^+$ boutons in apposition to the somata and the proximal 100 μm of in-plane dendrites of ChAT$^+$ motoneurons (10.0 ± 5.3, n = 140 boutons on 14 motoneurons; Figure 2E; Figure S2A for cervical motoneurons). To explore whether vGluT2$^+$/YFP$^+$ boutons originated from supraspinal YFP$^+$ neurons, we transected the spinal cords of *Isl1*-YFP mice (n = 2) at the thoracic level, and the animals were examined 7 days later. The density of vGluT2$^+$/YFP$^+$ boutons on motoneuronal somata and the proximal 100 μm of in-plane dendrites (6.6 ± 4.1, n = 93 boutons on 14 motoneurons) was similar to that found in nonspinalized mice (p = 0.07; Figure 2F), excluding the possibility that YFP$^+$ boutons contacting motoneurons derive primarily from supraspinal neurons. Rabies virus *trans*-synaptic tracing has also identified dI3 INs as a source of synaptic input to motoneurons (Stepien et al., 2010). Thus, glutamatergic dI3 INs project directly to motoneuron somata and dendrites (Figure 2G).

vGluT2$^+$/YFP$^+$ boutons were also detected in intermediate laminae of cervical and lumbar segments (12.8 ± 4.1 boutons/1,000 μm$^3$, n = 5 sections from 2 spinal cords; Figure S2B).

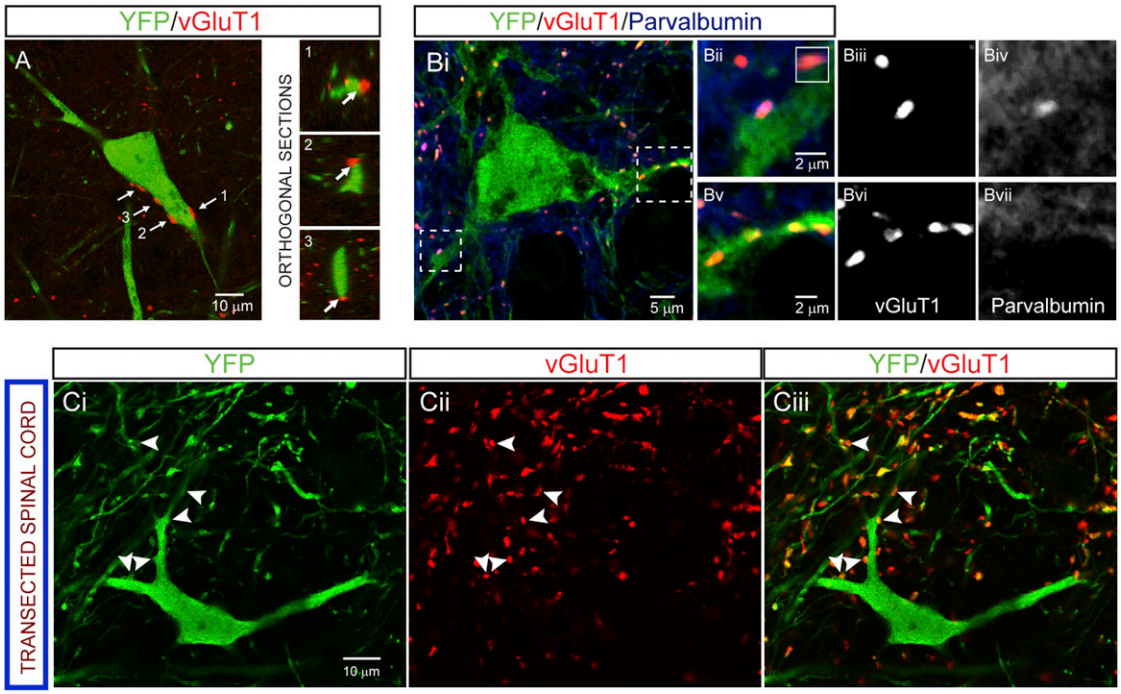


**Figure 3. Anatomical Evidence that Primary Afferents Project to dI3 INs**

(A) Left, a YFP$^+$ dI3 IN with vGluT1$^+$ boutons apposed (labeled by arrows). Right, Orthogonal sections confirming apposition of boutons labeled 1–3.

(B) vGluT1$^+$ boutons that are PV$^+$ and PV$^{null}$ on a YFP$^+$ dI3 IN from a P7 spinal cord. Boutons in dashed boxes are magnified in (Bii)–(Bvii). The inset in (Bii) depicts orthogonal sections of the PV$^+$/YFP$^+$ bouton in the Y-Z plane.

(C) vGluT1$^+$ boutons (arrowheads) on YFP$^+$ dI3 IN from a chronically transected spinal cord confirm that the boutons do not originate from supraspinal descending inputs.

All images are from *Isl1*-YFP mice.

Some of these boutons were in apposition to other dI3 INs (Figure S2C). Thus, both motoneurons and INs are targets of dI3 INs.

## dI3 INs Receive Monosynaptic Sensory Input

We determined whether dI3 INs receive direct input from primary sensory afferents. Expression of vGluT1 marks low-threshold cutaneous and proprioceptive primary afferent fibers and is excluded from spinal interneurons (Alvarez et al., 2004; Oliveira et al., 2003; Todd et al., 2003). We used vGluT1 as a molecular marker of direct afferent input to dI3 INs (Figure 3A). We found that 88% of YFP$^+$ dI3 INs (n = 46 out of 52 neurons) were contacted by vGluT1$^+$ boutons (9.2 ± 3.7 boutons /dI3 IN soma and proximal dendrites, n = 18). In the early postnatal spinal cord, parvalbumin (PV) serves as a marker of proprioceptive afferents (Mentis et al., 2006). Both vGluT1$^+$/PV$^+$ (n = 26) and vGluT1$^+$/PV$^{null}$ boutons (n = 85) were detected on dI3 INs at P1–P7 (n = 21, one to four optical sections per neuron were analyzed; Figure 3B). Thus, proprioceptive and cutaneous sensory afferents converge on dI3 INs. Analysis of vGluT1 labeling in adult spinal cord tissue examined 7 days after thoracic spinalization (n = 2) revealed no diminution in the number of vGluT1$^+$ boutons apposed to dI3 INs (n = 18 dI3 INs, 11.9 ± 8.0 boutons /dI3 IN, p = 0.2; Figure 3C), which was consistent with the view that these boutons derive from sensory afferents.

We used whole-cell patch-clamp recordings to assess the physiological connectivity between sensory afferents and dI3 INs. All dI3 INs in P5–P16 *Isl1*-YFP mice (n = 51, input resistance = 626 ± 356 MΩ) discharged repetitively. However, approximately one-sixth did not fire until after a delay of >50 ms because of the expression of a 4 AP-sensitive slowly inactivating potassium ($I_D$-type) current (Figures 4A and S3). Thus, transient synaptic excitation could elicit spike firing in most (approximately five-sixths) dI3 INs.

Then, we assessed sensory input using electrical stimulation of L4 or L5 dorsal roots, and this revealed that 105 out of 114 (92%) dI3 INs had sensory-evoked excitatory responses (Figure 4B). Of these 105 dI3 INs, 31 (30%) responded with a single excitatory postsynaptic potential (EPSP) or action potential, and 35 (33%) responded with a pattern comprised of an early EPSP or action potential followed by a longer-lasting IPSP (Figure 4Bi). The remaining 39 (37%) neurons responded with a sustained membrane depolarization that conferred repetitive firing in response to brief dorsal root (DR) stimulation (Figure 4Bii). Voltage-clamp recordings of responses to DR stimulation demonstrated CNQX-sensitive, multiphasic excitatory postsynaptic currents (EPSCs) of up to several hundred pAs (Figures 4C–4D; n = 5), and reversal potentials were near 0 mV (Figure 4E; n = 3). Thus, dI3 INs receive strong glutamatergic inputs from primary sensory afferents, which, in some cases, are mixed with longer latency excitatory and/or inhibitory inputs.

We measured the latency and jitter (Vrieseling and Arber, 2006) of dorsal-root-evoked EPSCs (drEPSCs) to determine

whether early responses were monosynaptic. The onset latencies of drEPSCs in dI3 INs from P5–P16 *Isl1*-YFP mice ranged from 2.0 to 20.0 ms. Latencies of known monosynaptic responses—ventral root reflexes and low-threshold, sensory-evoked EPSCs in motoneurons—were in the order of 2.0–2.5 ms (Figures 4Fi). drEPSC latencies below 3 ms were considered monosynaptic and were detected in 51 of 105 dI3 INs (Figures 4Fi and 4Gi). Both low and high jitter responses were seen (Figures 4Fii–4Fiii). A variance below 0.01 $ms^2$ was taken as indicative of monosynaptic input (Doyle and Andresen, 2001). Responses in 36 of 105 dI3 INs met this criterion (Figure 4Gii). Based upon these stringent criteria for latency and jitter, 32 of 105 (30%) dI3 INs received clear monosynaptic sensory input. The mean drEPSC latencies and jitters decreased with postnatal age (Figure 4Giii; see Jennings and Fitzgerald, 1998, and Mears and Frank, 1997), suggesting that this is an underestimate of what would be found in mature mice. Thus, dI3 INs receive monosynaptic input from sensory afferents.

To probe the class of sensory afferents that synapse on dI3 INs, we stimulated DRs with increasing stimulus intensities. Although stimulation of different afferent types can be controlled in the adult cat by the strength of stimulation, similar thresholds have not been established in young mice. Nevertheless, fibers would be recruited in order on the basis of their diameters and states of myelination (Erlanger and Gasser, 1930). Because of ongoing myelination and changes in thresholds and conduction velocities during earlier postnatal stages (Lizarraga et al., 2007), we restricted this analysis to recordings of dI3 INs between P12 and P16 (Figure 4H). Stimulation intensities were graded and are reported as factors of threshold (T) for evoking a monosynaptic ventral root reflex. Regardless of latency or the jitter level of response, every dI3 IN responded to low-threshold stimulation (n = 19). A quarter of these dI3 INs (n = 5 of 19) responded solely to low-threshold stimulation, whereas the remaining three-fourths also responded to medium- and/or high-threshold stimuli (Figure 4Hiii). These findings parallel the different molecular labeling of primary afferent boutons apposing dI3 INs (above; Figure 3C) and support the view that dI3 INs integrate a number of sensory modalities, including proprioceptive and low-threshold cutaneous afferents. Along with the evidence that dI3 INs project directly to motoneurons, these data suggest that dI3 INs are involved in low-threshold disynaptic reflex pathways (Figure 4I).

### dI3 INs Mediate Disynaptic Cutaneous-Evoked Reflexes

To examine the function of dI3 INs, we used genetic techniques to eliminate glutamate output from their terminals by crossing *Isl1*$^{+/Cre}$ mice to *vGluT2*$^{flox/flox}$ mice (dI3$^{OFF}$ mice; Figure 5A). To confirm an effective reduction in glutamatergic capacity, we asked (a) whether *vGluT2* messenger RNA (mRNA) expression is reduced or eliminated in dI3 INs, (b) whether vGluT2 protein is eliminated from the boutons of dI3 INs in apposition to MNs, (c) whether low threshold primary afferent input to dI3 INs is unaffected, and (d) whether sensory receptors or motoneurons are affected.

In dI3$^{OFF}$ mice, traces of *vGluT2* mRNA were detected in only 28% of dI3 INs (n = 91 of 330 neurons in 2 mice, P13–P20; Figure 5B). Second, YFP$^{+}$ dI3 INs still projected to motoneurons (Figure 5C), but there was a 93% reduction in vGluT2$^{+}$/YFP$^{+}$ boutons in apposition to ChAT$^{+}$ motoneuronal somata and proximal 100 μm of dendrites in plane (0.7 boutons/motoneuron, n = 10 motoneurons, P13–P20; Figure 5D). Third, primary afferent inputs to dI3 INs were unaffected in dI3$^{OFF}$ mice, as demonstrated both immunohistochemically (eight out of nine dI3 INs, 8.8 ± 7.3 vGluT1$^{+}$/YFP$^{+}$ boutons per dI3 IN, P13–P20; Figure 5E) and electrophysiologically (drEPSCs were seen in eight out of ten dI3 INs from P13–P14 dI3$^{OFF}$ mice, similar to the frequency seen in *Isl1*-YFP mice, chi-square test, p = 0.2; in four of these eight dI3 INs, these EPSCs met strict short-latency, low-jitter thresholds, similar to the five out of eight cells seen in *Isl1*-YFP at similar age range, chi-square test, p = 0.6; Figure 5F). Moreover, normal sensory-evoked monosynaptic reflexes were recorded from ventral roots (Figure 5F), suggesting that vGluT1 function was not altered in primary afferents. Fourth, the expression of vGluT2 in Merkel cells, cutaneous transduction cells that express Isl1 and mediate low-threshold mechanical input from the paws (Haeberle et al., 2004; Maricich et al., 2009), was unaffected in dI3$^{OFF}$ mice (Figure S4A). In addition, there were no changes in mechanical nociception, as assessed by von Frey hair testing in these mutant mice (Figure S4C). Finally, no motoneuronal dysfunction was found; there was no apparent weakness during treadmill walking (data not shown), and no alterations in motor responses (M-waves) or monosynaptic reflexes (H-reflexes; see below). Altogether, these data suggest that the primary consequence of the genetic manipulation used to make dI3$^{OFF}$ mice is not a dysfunction of the afferent system but is rather a loss of glutamatergic output of dI3 INs.

To assess whether there was cutaneous afferent input to dI3 INs, we labeled afferents of the sural nerve and detected boutons in apposition to dI3 INs (Figure 6A; n = 3). Then, we used sural nerve stimulation in neonatal and adult preparations in dI3$^{OFF}$ and control mice to assess this putative disynaptic pathway. Stimulation of the sural nerve in in vitro preparations (P1–P3; Figure 6C) led to L5 DR volleys of longer delay (1–2.5 ms, n = 5; Figure 6D) than those obtained with tibial nerve stimulation, which was consistent with slower conduction velocities in cutaneous afferents compared to muscle afferents. The thresholds for eliciting these responses were similar for the two nerves, (2–4 μA), demonstrating that, although we could not be specific about the fiber type stimulated, we were using the lowest possible currents to evoke responses.

Next, we assessed disynaptic reflex responses. The latencies of ventral root reflexes in response to sural nerve stimulation were 4–5 ms (n = 3) longer than their latencies in response to tibial nerve stimulation (Figure 6E), which was reflective of the fact that tibial nerve stimulation elicits monosynaptic, Ia afferent-evoked reflexes and suggests that the reflex evoked by sural nerve stimulation involves one to two additional synapses (Figure 6B). The stimulation thresholds for eliciting short-latency reflexes by sural nerve stimulation ranged from 1.5–2 T (n = 5), where T is defined as the smallest stimulation strength at which a DR volley was seen. This suggests that the short-latency response from sural nerve stimulation is mediated by cutaneous afferents, possibly ones with low thresholds.

In dI3$^{OFF}$ mice, DR volleys in response to sural nerve stimulation were similar to those in control mice (Figure S5A), but the mean–normalized, short-latency ventral root response was

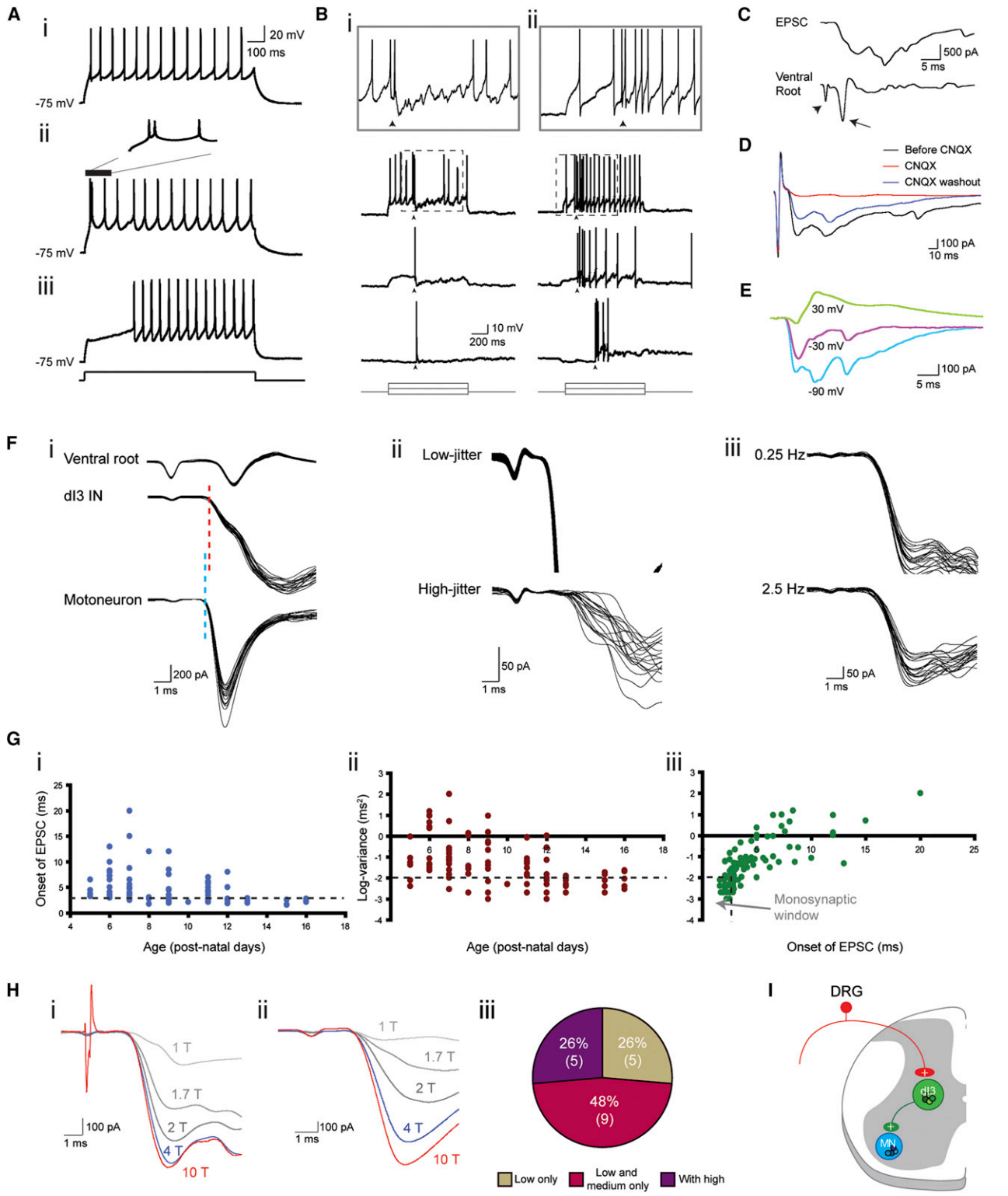


**Figure 4. Response of dI3 INs to Sensory Afferent Stimulation**

(A) Three types of firing behaviors: (i) tonic firing, (ii) initial bursting, and (iii) delayed firing.

(B) Current-clamp recording of two dI3 INs showing response to DR stimulation (20 μA, just under 3 × T, 250 μs) during the current steps of three different magnitudes. (i) A cell responding with an action potential followed by a prolonged hyperpolarization; (ii) a cell responding with a prolonged depolarization. Arrowheads mark the time of stimulation. The top row is a scaled version of the area marked by dashed box in second row.

*(legend continued on next page)*

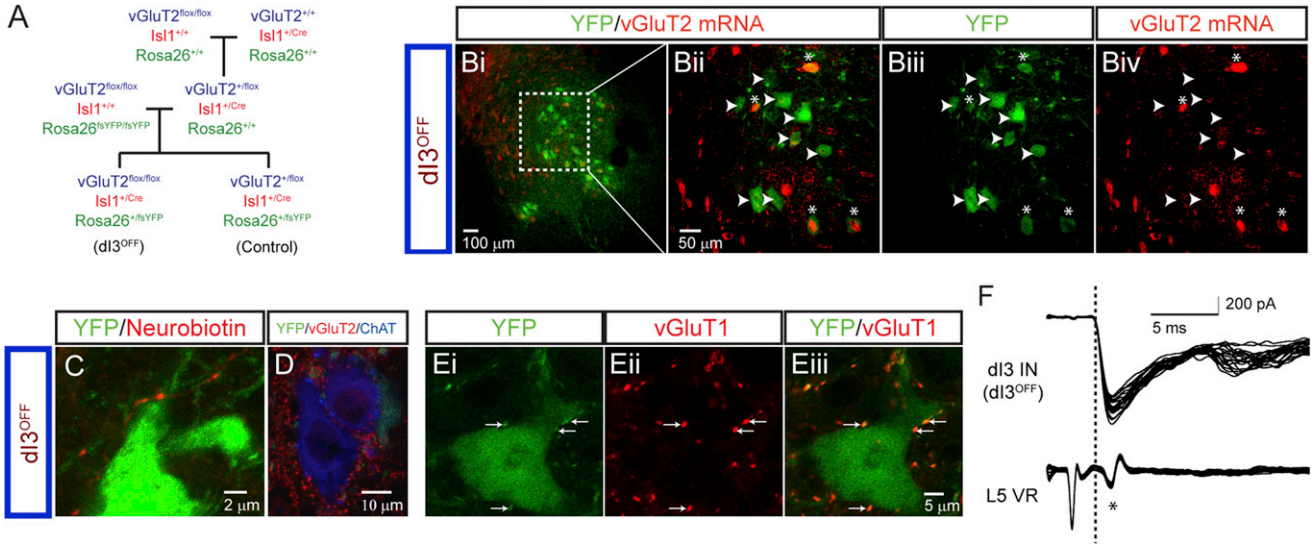


**Figure 5. Loss of vGluT2 Expression in dI3$^{OFF}$ Mice**

(A) A breeding strategy to generate the silencing of the output of dI3 INs (dI3$^{OFF}$) by conditionally knocking out vGluT2. fsYFP refers to *loxP-stop-lox-YFP*. Only the genotypes that were used are shown.

(B) Fluorescent in situ hybridization shows the presence of *vGluT2* mRNA reduced to 28% of YFP$^{+}$ dI3 INs, (n = 92 out of 330 neurons from two mice) in dI3$^{OFF}$ animals. Asterisks denote dI3 INs with the presence of *vGluT2* mRNA. Arrowheads denote dI3 INs in the absence of *vGluT2* mRNA.

(C) After neurobiotin injection in a dI3 IN from a dI3$^{OFF}$ animal, bouton-like appositions are present on a putative YFP$^{+}$ motoneuron in lamina IX.

(D) Loss of vGluT2$^{+}$/YFP$^{+}$ boutons on the ChAT$^{+}$ motoneuron.

(E) vGluT1$^{+}$ inputs to YFP$^{+}$ dI3 INs are still present in dI3$^{OFF}$ mice (8/9 dI3 INs).

(F) Ventral root reflex and monosynaptic dorsal root-evoked EPSCs in dI3 INs are present in dI3$^{OFF}$ mice (eight out of ten dI3 INs showed dorsal root-evoked EPSCs; four out of ten dI3 INs met strict short-latency, low-jitter thresholds, as above). Interestingly, these mice became pruritic (Figure S4B), which might be expected after a loss of vGluT2 from high-threshold afferents (Lagerström et al., 2010; Liu et al., 2010).

All images are from the lumbar spinal cord of P13–P16 dI3$^{OFF}$ mice. See also Figure S4.

significantly smaller ($p < 0.05$; Figure 6F) in dI3$^{OFF}$ mice (1.1 ± 0.3, mean ± pooled SD, n = 4) in comparison to control mice (3.2 ± 0.8, n = 7). The short-latency reflexes were present in six of seven control animals, as opposed to zero of four dI3$^{OFF}$ animals ($p < 0.05$, chi-square test), indicating that dI3 INs mediate a short-latency response, which is most likely a disynaptic cutaneous to motor reflex in neonatal mice.

To determine whether dI3 INs mediate this reflex in awake adult mice (Figure 6G), we ensured that monosynaptic reflexes were not affected in dI3$^{OFF}$ mice. Single-pulse tibial nerve stimulation (Figure 6Hi) produced both a direct M-wave and an H-reflex response (latency in the range of 2–3 ms; Figure 6Hii). Both the M-wave and H-reflex were observable in control and in dI3$^{OFF}$ animals, and the ratios of H-reflex to M-wave,

(C) Voltage-clamp recording of L5 dI3 IN depicting an EPSC in response to DR stimulation (20 μA, just under 3 × T, 250 μs) with an accompanying extracellular ventral root (L5) recording. The arrowhead marks the stimulation artifact, whereas the arrow marks the monosynaptic ventral root response.

(D) EPSCs in response to DR stimulation (20 μA, just under 3 × T) reversibly blocked by CNQX.

(E) drEPSCs at different holding potentials showing the reversal of EPSC at the depolarized potential.

(F) A demonstration of monosynaptic nature of sensory input. (i) The onset of drEPSC (15 μA, 3 × T) in dI3 IN, as compared to the onset of monosynaptic EPSC in a motoneuron from the same preparation. These two cells were recorded separately. The ventral root recording was concomitant with the motoneuron recording. The timing of the ventral root response during dI3 IN recording was the same. The blue dashed line marks the onset of the motoneuron EPSC. The red dashed line marks the onset of the dI3 IN EPSC. The difference was below 0.2 ms. (ii) drEPSCs (15 μA, 3 × T) in dI3 IN with low jitter (0.002 ms$^2$, jitter was calculated on 20 responses) (top); drEPSCs (20 μA, 4 × T) in dI3 IN with high jitter (0.47 ms$^2$) (bottom). (iii) Low-latency, low-jitter drEPSCs in dI3 IN with no failures in response to 0.25 and 2.5 Hz stimulation frequency (n = 3), confirming these are monosynaptic responses.

(G) A shift toward monosynaptic sensory inputs with age is shown. The relation between (i), onset of drEPSC in dI3 INs and age, (ii), variance of drEPSC onset and age, and (iii), variance of drEPSC onset and onset of drEPSC.

(H) Response to different strengths of DR stimulation. (i) dI3 IN with increases in drEPSC magnitude with a shift from low to medium strength but not to high-threshold dorsal root stimulation. (ii) dI3 IN with increases in drEPSC magnitude with shift from low- to medium- to high-threshold dorsal root stimulation. T refers to the threshold at which a monosynaptic ventral root reflex was elicited. (iii) The distribution of sets of responses in dI3 INs to DR stimulation (single 250 μs pulses). Low-threshold fibers were considered to be recruited by stimulation between 1–2 × T, medium-threshold fibers were recruited by 2–5 × T, and high-threshold fibers were recruited by stimulation above 5 × T. T is the earliest stimulation strength at which a monosynaptic ventral root reflex was elicited in ventral roots. The number of cells is shown in parentheses.

(I) A diagram representing dI3 INs as part of a disynaptic pathway between sensory input and motoneurons.

See also Figure S3.

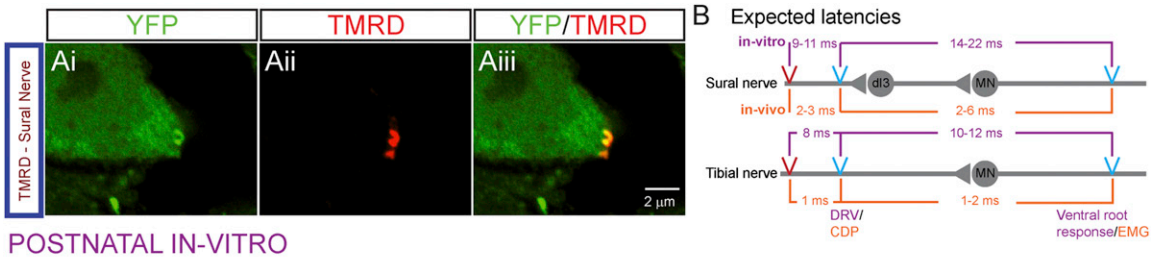


POSTNATAL IN-VITRO

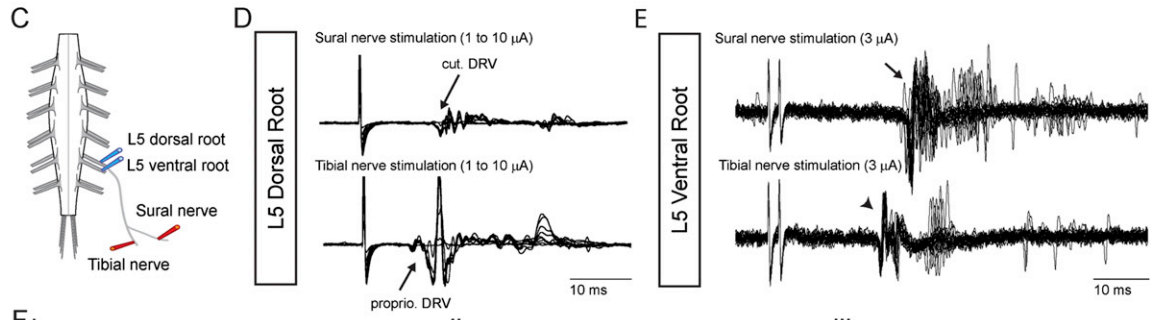


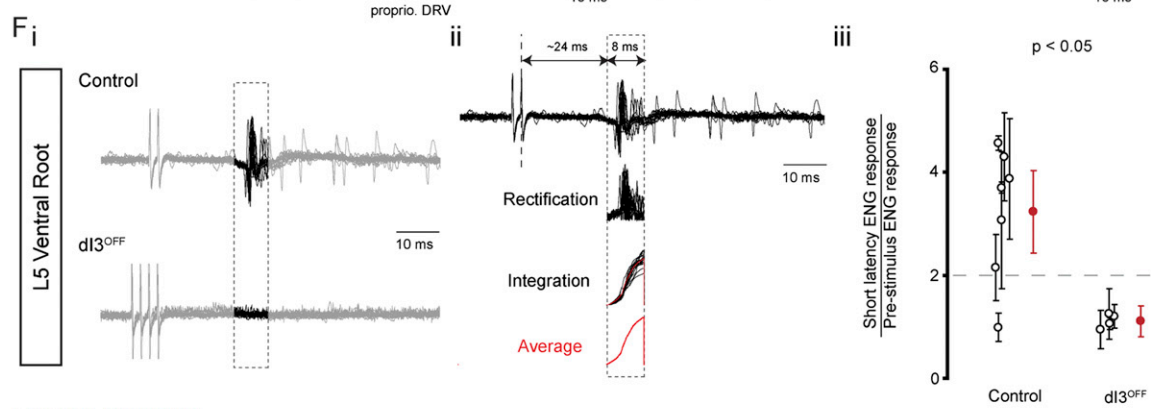


ADULT IN-VIVO

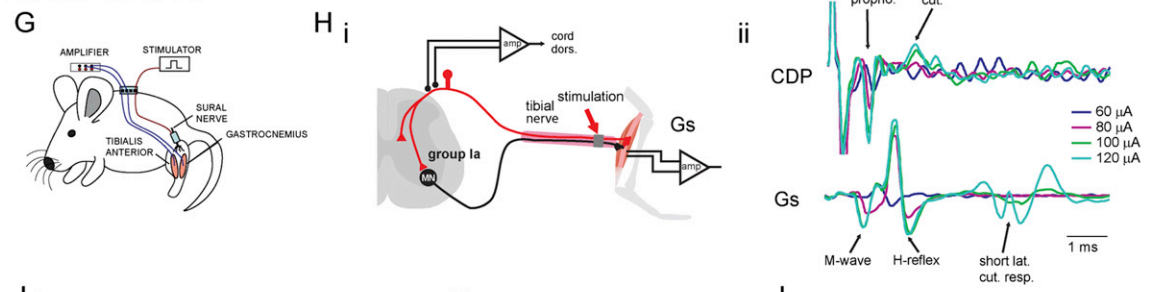


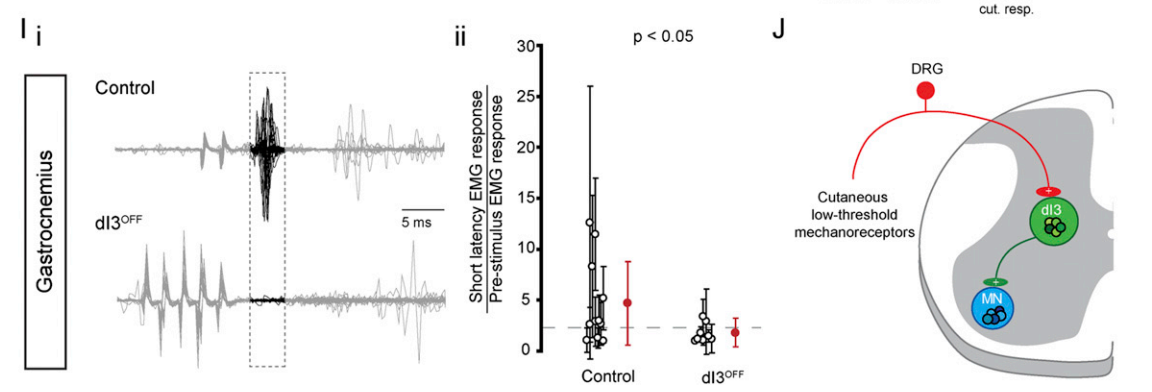


(legend on next page)

calculated at 2 T, were similar ($p = 0.2$) in controls (0.19 ± 0.06, $n = 3$) and mutants (0.30 ± 0.16, $n = 4$), which was indicative of normal Ia afferent reflexes and motoneuron activity in dI3$^{OFF}$ mice.

To test short-latency reflexes evoked by sural nerve stimulation, we ensured that we were not stimulating high-threshold sural nerve afferents by adjusting the stimulation strengths to the range at which short-latency responses were first seen in cord dorsum potential (CDP) recordings ($n = 1$ control and 2 dI3$^{OFF}$ animals; Figures 6H and S5B). These stimuli were below nociceptive thresholds, as determined by vocalizations. Sural nerve stimulation did not produce short-latency responses in tibialis anterior (TA) in either control or mutant mice. However, a short-latency reflex was present in gastrocnemius (Gs) in 8 of 11 control mice, as compared to only two of eight dI3$^{OFF}$ mice (chi-square test, $p < 0.05$), despite the use of multiple shocks in potentiating the response (Figure 6Ii). The mean-normalized EMG response was 1.8 ± 1.4 (mean ± pooled SD) in dI3$^{OFF}$ mice ($n = 8$) in comparison to 4.1 ± 3.5 in control littermates ($n = 11$, $p < 0.05$; Figure 6Iii). This loss or reduction of motor response to sural nerve stimulation in dI3$^{OFF}$ mice indicates that dI3 INs mediate a short-latency, low-threshold cutaneous-motor reflex (Figure 6J).

## dI3 INs Are Necessary for Normal Grip Function

To assess how silencing the output of the dI3 INs affects motor tasks that require cutaneous afferent feedback, we tested the performance of mutants with a locomotor task. On a horizontal ladder with uniform spacing between rungs, the number of hindlimb missteps was greater in dI3$^{OFF}$ mice (control, 2.8 ± 3.0 slips per 100 steps; dI3$^{OFF}$, 9.2 ± 5.7 slips per 100 steps; $p < 0.05$; Figure 7A). In addition, falls from the ladder were occasionally observed during the testing of dI3$^{OFF}$ mice but never with control littermates. This suggests that hindlimbs rely on dI3 INs to ensure appropriate grip of the ladder rungs during ladder walking.

To explore the functional consequence of eliminating dI3 IN output further, we turned to a paw grip task that involved low-threshold cutaneous receptors (Witney et al., 2004). Both control and dI3$^{OFF}$ adult mice attempted to grasp the metal bars (indicating that they could sense the bars), but the volar surfaces (forelimb and hindlimb) of the paws of dI3$^{OFF}$ mice did not fully grip the bars (Figure 7B). During slow inversion of the cage top, the dI3$^{OFF}$ mice would slide down the grid because of an apparent failure to maintain adequate grip strength (Movie S1). The angle at which the dI3$^{OFF}$ mice were unable to remain on the cage top was 58° ± 12° from the horizontal axis (mean ± pooled SD; $n = 3$ trials for three mice; Figure 7C). When the grid was inverted to angles beyond vertical, dI3$^{OFF}$ mice were unable to hang onto the grid ($n = 10$ out of ten, three trials each; seven males, three females; P30–P120; Figure 7D and Movie S1). Control littermates could hang on for long periods averaging 50 s per trial ($n = 12$ out of 12, three trials each; four males, eight females; P30–P120; Figure 7D and Movie S2). These data suggest that the silencing of the output of dI3 INs impairs grasping and the ability to regulate grip strength in the face of an increasing load.

To determine whether the loss of grip function resulted from dysfunction within the spinal cord, we studied the forepaw grasp reflex in neonatal animals at an age prior to maturation of descending systems (Amendola et al., 2004; Fox, 1965). Although 35 of 36 control pups (P1–P7) had reflexive palmar flexion in response to gentle stroking of the palmar surface, a stimulus that would activate low-threshold mechanoreceptors, only 2 of

**Figure 6. Conditional Silencing of the Output of dI3 INs Abolishes Short-Latency Response to Cutaneous Nerve Stimulation**

(A) Tetramethylrhodamine (TMRD)$^{+}$ boutons on a YFP$^{+}$ dI3 IN in an *Isl1*-YFP spinal cord 3 days after TMRD labeling of the sural nerve, a predominantly cutaneous nerve (Peyronnard and Charron, 1982).

(B) A schematic describing the estimated latencies of monosynaptic and disynaptic ventral root reflexes in response to tibial and sural nerve stimulation, respectively. Estimates were calculated for experiments with postnatal isolated spinal cord preparations with the sural nerve in continuity and adult in vivo recordings and were based upon the observed latencies between stimulation, DR volley or CDP, and ventral root reflexes or EMG recordings.

(C) A scheme of isolated spinal cord preparation with the sural nerve left in continuity. Stimulating electrodes were placed on the sural nerve and the tibial nerve distal to the sural nerve branchpoint. Recording electrodes were placed on the ipsilateral L5 dorsal and ventral roots.

(D) L5 dorsal root potentials in response to sural nerve or tibial nerve stimulations. In this example, the earliest DR volley to the sural and tibial nerve stimulations were seen at 3 and 2 μA, respectively.

(E) Shown are 20 traces of L5 ventral root reflexes elicited by two 250 μs shocks (500 Hz) applied to the sural and the tibial nerve. Note the low-jitter monosynaptic reflex in response to tibial nerve stimulation (arrowhead) versus the high-jitter short-latency oligosynaptic reflex in response to sural nerve stimulation (arrow).

(F) (i) Recordings of L5 ventral root ENGs to multiple stimulation pulses applied to the sural nerve. Putative disynaptic reflex responses are highlighted in the dashed box. (ii) The methodology for the quantification of short-latency response in an 8 ms time window, 14 ms from low-threshold L5 DR volley from sural nerve stimulation (not shown). (iii) A summary of short-latency L5 ventral root ENG reflex response to sural nerve stimulation. The data point shows the ratio of the time-integrated ENG response to sural nerve stimulation in the short-latency ENG time window over the time-integrated ENG response in a randomly selected 8 ms time window prior to the application of the stimulus trains. Clear circles represent each isolated spinal cord, and filled circles represent the group average. Error bars represent SD. The dashed line represents a reflex ratio threshold of 2.

(G) A scheme of EMG recordings of chronically implanted electrodes into Gs and TA muscles of control and dI3$^{OFF}$ mice.

(H) Recordings of cord dorsum potentials (CDPs) in response to tibial nerve stimulation. (i) Recording setup. (ii) CDP showing the activation of proprioceptive and cutaneous potentials with increasing current stimulation (top); corresponding EMG recording of Gs (bottom).

(I) (i) Recordings of Gs EMG to multiple stimulation pulses applied to the sural nerve. Putative disynaptic reflex responses are highlighted in the dashed box. (ii) A summary of short-latency synaptic EMG response reflex response measured in a 4 ms time window, 4 ms after the onset of the last stimulation pulse to sural nerve stimulation. The data point shows the ratio of the time-integrated EMG response to sural nerve stimulation in the short-latency EMG time window over the time-integrated EMG response in a randomly selected 4 ms time window prior to the application of the stimulus trains. Clear circles represent each animal, and filled circles represent the group average. Error bars represent SD. The dashed line represents a reflex ratio threshold of 2.

(J) A diagram representing dI3 INs as part of a disynaptic pathway between low-threshold mechanoreceptors from the skin and motoneurons.

See also Figure S5.

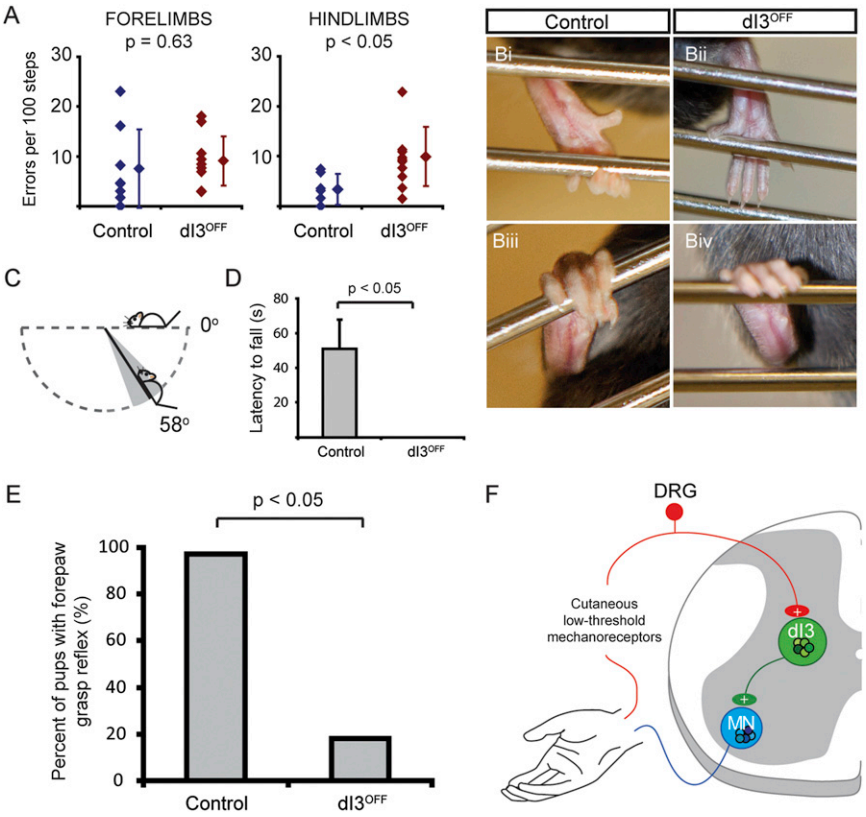


**Figure 7. Reduced Performance in Several Motor Tasks Involving Cutaneous Afferents from the Paw, Including Loss of Functional Grip in dI3$^{OFF}$ Mice**

(A) During ladder walking with a rung spacing of 2 cm, forelimb errors are similar in controls and mutants, whereas the mutants have more hindlimb errors than controls. Error bars represent SD.

(B) A comparison of the hindlimb grip of a metal bar for control and dI3$^{OFF}$ mice.

(C) A diagram depicting the minimal angle from the horizontal axis at which dI3$^{OFF}$ mice are unable to hang onto the cage top. In the wire hang test, control animals grip onto the cage top while upside down for close to 1 min, whereas the dI3$^{OFF}$ mice are unable to hang onto the cage top while inverted. The gray cone represents the pooled SD.

(D) Performance of control and dI3$^{OFF}$ mice during the wire hang test. The maximal duration of the test was 1 min. Every control animal would hang on for periods longer than 1 min in at least one of the three trials. Similar results were observed when mice were tested a second time 1 or two 2 later. Error bars represent SD.

See also Movies S1 and S2.

(E) Absence of the forepaw grasp reflex in dI3$^{OFF}$postnatal (P1–P7) mice, as indicated by a chi-square test.

(F) A diagram representing dI3 INs as part of a disynaptic pathway between low-threshold mechanoreceptors from the skin and motoneurons involved with regulating grip strength.

11 dI3$^{OFF}$ mutant pups exhibited this grasp reflex (Figure 7E; chi-square test, $p < 0.05$). Altogether, these behavioral experiments provide evidence that spinal microcircuits involving dI3 INs mediate disynaptic reflex pathways from low-threshold cutaneous afferents to motoneurons (Figure 7F) and play key roles in motor behaviors that involve cutaneous afferent feedback—notably the regulation of forelimb and hindlimb grip strength.

## DISCUSSION

The spinal cord contains the neural circuitry necessary to produce a wide range of motor behaviors. However, the roles of particular neurons and their microcircuits in the execution of motor behaviors are poorly understood. We have identified a class of spinal interneurons, dI3 INs, that participate in a microcircuit necessary for cutaneous regulation of motor output. We show that dI3 INs mediate a disynaptic cutaneous-motor reflex circuit and that this microcircuit is critical for the normal regulation of grasping in response to a changing environment. Thus, dI3 INs form spinal microcircuits necessary for this specific motor behavior.

### dI3 INs Are Involved in a Disynaptic Cutaneous-Motor Microcircuit

Studies of sensory-motor control in primates, including humans, have largely focused on the role of cutaneous inputs in forelimb, in particular hand, function (Witney et al., 2004). Insights from these studies have revealed that hand function is reliant on cutaneous input. However, the spinal circuits involved in cutaneous-motor control of hand function have not been defined. We used knowledge of the molecular development of the mouse spinal cord that has been useful for genetic characterization of spinal locomotor circuits (Grossmann et al., 2010; Kiehn, 2011) to address microcircuits involved in the sensorimotor integration necessary for hand function.

The loss of a cutaneous-motor reflex in dI3$^{OFF}$ mice resulted from the functional loss of the internuncial neurons (dI3 INs) in the reflex pathway resulting from the deletion of vGluT2. The reflex or behavioral deficits observed in dI3$^{OFF}$ mice would not have resulted from the deletion of vGluT2 from primary afferents, given that, in the spinal cord, large-diameter primary afferents originating from proprioceptors and low-threshold mechanoreceptors express vGluT1, whereas vGluT2 is confined to small diameter afferents from high-threshold nociceptors (Alvarez et al., 2004; Brumovsky et al., 2007; Landry et al., 2004). Furthermore, we demonstrate that, in dI3$^{OFF}$ mice, low-threshold afferent input to dI3 INs is not affected, whereas cutaneous short-latency reflex pathways are disrupted. Although we detected traces of *vGluT2* mRNA in about one-quarter of dI3 INs in dI3$^{OFF}$ mice, 93% of dI3 axon boutons in motor pools were devoid of vGluT2 protein, indicating that this was an effective strategy to reduce neurotransmission from dI3 INs. Altogether, this indicates that the deficit in the reflex pathway was the elimination of vGluT2 in dI3 INs and, hence, the output from dI3 INs to motoneurons. In summary, the preservation of input to dI3 INs, the loss of vGluT2 in dI3 IN boutons in motor pools, along with

the loss of reflex responses in short-latency time windows in dI3$^{OFF}$ mice suggests that the same interneurons that receive cutaneous inputs project to motoneurons, forming a disynaptic cutaneous sensory-motor microcircuit.

## dI3 INs as Mediators of Grip Control

The elimination of vGluT2 from dI3 INs leads to the loss of a specific motor behavior —grasp—with minimal deficits in the other motor tasks studied. Although the deficit seen in the ladder task in dI3$^{OFF}$ mice suggests that dI3 INs integrate cutaneous input necessary for appropriate hindlimb placement, the most profound deficit was the inability of dI3$^{OFF}$ mice to regulate grip control. Whether the loss of grip function was solely due to the loss of functional output from dI3 INs to motoneurons and/or to interneurons in intermediate laminae remains unclear. Nevertheless, it is likely that dI3 INs are involved in the mediating haptic input necessary for many behaviors, and it is also likely that our assay—grip testing—reveals one clear deficit.

As with the loss of cutaneous-motor reflexes, the behavioral deficits in dI3$^{OFF}$ mice result from a functional deficit in dI3 INs. The behavior cannot be explained by the disruption of cutaneous Merkel cells, because the elimination of these sensory receptors does not lead to any deficit in the wire hang test (Maricich et al., 2012). Corresponding to this, the deletion of vGluT2 from various dorsal root ganglion neurons led to a reduction in thermal and/or mechanical nociception (Lagerström et al., 2010; Scherrer et al., 2010) and a deficit in the response to intense but not light mechanical stimulation (Liu et al., 2010). Deletion of vGluT2 from all sensory neurons (Lagerström et al., 2010; Pietri et al., 2003) did not result in any motor deficits, as assessed by rotarod, balance beam (Rogoz et al., 2012), or wire hang testing (K. Kullander, personal communication). Altogether, this indicates that the deficits observed were not related to deficits in the afferent system.

The involvement of dI3 INs in grasp circuitry is consistent with their role in mediating sensory information from cutaneous mechanosensitive receptors, which mediate their effects via low-threshold afferents. This afferent system plays a key role in mediating grip in humans (Dimitriou and Edin, 2008; Johansson and Flanagan, 2009). Humans cannot perform gripping tasks accurately after local anaesthetization of the fingers or hand (Augurelle et al., 2003; Johansson and Westling, 1984). As with dI3$^{OFF}$ mice, this deficit could not be compensated by feed-forward descending control; i.e., the required grip and load forces could not be accurately predicted (Monzée et al., 2003; Witney et al., 2004), and maximal attainable pinch force was reduced (Augurelle et al., 2003). Our findings indicate that, in mice, the cutaneous input necessary to regulate grip strength is processed in a spinal microcircuit involving dI3 INs.

Previous studies have examined supraspinal mechanisms involved in primate hand function (Baker, 2011; Fuglevand, 2011; Schieber, 2011), but the spinal circuits that mediate this goal-directed motor behavior are not understood. Grip types can be broadly divided into two categories: precision grip and power grip (Napier, 1956; Young, 2003). Recent studies have demonstrated that propriospinal neurons in C3 and C4 segments are critical for executing a reach-and-precision grip task in primates (Alstermark et al., 2011; Kinoshita et al., 2012), but the microcircuits regulating power grip, which require cutaneous feedback control so that grip can be adjusted to unexpected environmental cues (Witney et al., 2004), have not been previously defined. The spinal neurons that are responsible for regulating grip strength would be ideal candidates in mediating the integration of feedback and feed-forward commands to appropriately regulate grip strength. We have shown that dI3 INs process feedback signals and suggest that they may also integrate descending commands for grip.

## Evolutionary and Human Considerations

The development of the hand and foot and the concurrent development of their neural control circuits were key adaptations in evolution. Prior to the evolution of precision grip and fine finger movements, basic hand function—the power grip, in particular—provided significant evolutionary advantages. The ability of lizards to grip fine tree branches and rapidly release and regrip allowed them to navigate narrow branches (Abdala et al., 2009). These rather simple, yet important, grip functions predated the evolution of more complex grips in humans (Young, 2003) and would have required the development or exaptation of appropriate spinal control circuits. One candidate population from which dI3 INs could have developed are *Xenopus* tadpole dorsolateral ascending interneurons, because these are also glutamatergic, receive cutaneous inputs, and project to other spinal neurons (Li et al., 2004). In addition, nonhuman primate studies have demonstrated activity of spinal interneurons in a location similar to that of dI3 INs during grasp, suggesting that they may be responsible for combining and coordinating multiple hand muscles during tasks requiring precision grip (Takei and Seki, 2010). Interneurons in this intermediate region that are tuned to grip strength receive inputs from cutaneous afferents (Fetz et al., 2002) and multiple descending systems (Riddle and Baker, 2010). The similar locations and inputs of these interneurons in the mouse, cat, and monkey suggest that dI3 INs, which play a critical role in paw function, are conserved features of mammalian spinal cord organization.

We have described a spinal microcircuit in mice that underlies a disynaptic grasp reflex. The normal grasp reflex evoked by palmar cutaneous stimulation in the neonate is absent in the dI3$^{OFF}$ mice. Similarly, the activity of an orthologous spinal microcircuit may be responsible for the grasp reflex in the human infant. Human fetuses develop a grasp reflex in the first trimester (Hooker, 1938) that persists in the postnatal period for 2–6 months (Halverson, 1937; Pollack, 1960). Reflexive grasping is not normally seen in adult humans, most likely because higher systems regulate this microcircuit, which may also be involved in feed-forward control of hand function (see Rushworth and Denny-Brown, 1959). Presumably, these reflexes disappear because of the development of the brain and descending systems. Grasp reflexes emerge in adults with structural brain (Walshe and Hunt, 1936) and neurodegenerative diseases and their pathological reemergence can be quite disabling for both hand (Mestre and Lang, 2010) and foot function (Paulson and Gottlieb, 1968). In addition, the opposite effect—a loss of normal control of hand grasp, resulting, for example, from spinal cord injury—is significantly disabling (Anderson, 2004). Understanding dI3 INs and their control will aid

in the development of microcircuit-targeted therapies to improve hand dysfunction in disease or following injury.

## EXPERIMENTAL PROCEDURES

### Animals

Expression of YFP driven by the promoter for the homeodomain transcription factor Isl1 was obtained in double transgenic offspring of *Isl1*$^{+/Cre}$ and *Thy1-lox-stop-lox-YFP* mice.

The following strains of mice were generously donated and used in this study: *Thy1-lox-stop-lox-YFP* mice (from J. Sanes) and *Thy1-lox-stop-lox-mGFP* (from S. Arber). Conditional knockout of vGluT2 in Isl1-expressing neurons (dI3$^{OFF}$) was accomplished by crossing *Isl1*$^{+/Cre}$ mice with a strain of mice bearing a conditional allele of the *Slc17a6* (*vGluT2*) gene where exon 2 of the gene was flanked by *loxP* sequences (*vGluT2*$^{flox/flox}$; Figure 5A). This resulted in Cre-mediated excision of exon 2 of the *vGluT2* gene in Isl1-expressing neurons (Hnasko et al., 2010). All animal procedures were approved by the University Committee on Laboratory Animals of Dalhousie University and conform to the guidelines put forth by the Canadian Council for Animal Care. Additional methodological details can be found in Supplemental Information.

### Electrophysiology

#### *In Vitro Spinal Cord Preparations*

Sagittal hemicords were prepared from *Isl1*-YFP or dI3$^{OFF}$ postnatal (P5–P16) mice. After anesthesia was administered by an injection of a mixture of xylazine and ketamine, mice were decapitated, and spinal cords were isolated by vertebrectomy in room temperature recording artificial cerebrospinal fluid (ACSF) (NaCl, 127 mM; KCl, 3 mM; $NaH_2PO_4$, 1.2 mM; $MgCl_2$, 1 mM; $CaCl_2$, 2 mM; $NaHCO_3$, 26 mM; D-glucose, 10 mM). Ventral and dorsal roots were dissected as distally as possible. Cords were hemisected by a midline longitudinal incision, incubated for 45–60 min in 37°C recording ACSF, and equilibrated in room temperature recording ACSF for at least 30 min. Then, hemicords were pinned, medial side up, to a base of clear Sylgard (Dow Corning) and perfused with room temperature recording ACSF. Ventral and dorsal root activity was recorded via suction electrodes (A-M Systems). Fluorescent dI3 INs were targeted on the basis of their location in the intermediate spinal cord and recorded with care to not include cells that were deep (motoneurons). Most recordings were from L4 and L5 segments, but, when recording in rostral lumbar segments, neurons near the surface (possible autonomic motoneurons) were also avoided.

#### *Electrophysiological Testing of Sensory Inputs*

Sensory fibers have different recruitment thresholds, which depend on the size of the fiber and the degree of myelination (Erlanger and Gasser, 1930). To express stimulation strength, we defined T as either the lowest stimulus strength at which DR volleys or CDPs were first seen (if electrodes present) or the strength at which ventral root responses were seen. We classified the responses of dI3 INs as either low-threshold (1–2 T), which would include group I muscle afferents and low-threshold cutaneous afferents (Aβ) but also some group II and Aδ fibers, or high-threshold afferents (5–10 T), which putatively included group III and group IV muscle afferents and unmyelinated C fiber nociceptive afferents. Intermediate stimuli were classified as medium threshold. T was typically between 4 and 20 μA in vitro.

#### *In Vivo Measurement of EMG Response to Nerve Stimulation*

Adult mice were implanted with bipolar electromyography (EMG)-recording electrodes (Pearson et al., 2005; Akay et al., 2006) as well as cuff electrodes to stimulate the tibial and/or sural nerves. Following 1–3 weeks of recovery, nerves were stimulated with the use of single or pairs of 250 μs pulses for the tibial nerve or with the use of trains of two to five pulses for the sural nerve at frequencies of 500 Hz with an interval of 2 s between trains. Stimulation strengths used to attempt to elicit reflexes ranged between 75 and 500 μA (mean, 307 ± 135 μA; n = 11) in the control animals and 40 to 750 μA (mean, 248 ± 228 μA; n = 8) in the mutant animals ($p = 0.31$). In contrast, the nociceptive threshold (producing vocalizations) ranged between 300 and 1,500 μA (mean, 821 ± 356 μA; n = 7) in the control animals and between 250 and 900 μA (mean, 571 ± 216 μA; n = 7) in the mutant animals ($p = 0.07$). The differences between the stimulation used to elicit the short-latency reflexes and the threshold for vocalization were significant (paired t test, $p < 0.05$, n = 5 control and 2 dI3$^{OFF}$ animals). We implanted chronic epidural cord dorsum electrodes in four animals to determine stimulation thresholds (n = 2 mutant and 2 controls). The threshold to elicit short-latency cord dorsum responses from sural nerve stimulation was between 100 and 300 μA (Figure S5B; n = 2 mutants and 1 control); i.e., in the same range that we used to elicit reflex responses.

### Reflex Quantification

To quantify putative disynaptic responses in vitro, we rectified recordings and integrated them in a time window from 14–22 ms after the onset of the DR volley (Figure 6B), and the recordings were expressed as a ratio of the prestimulus integrated voltage.

In vivo, EMG responses were similarly quantified in a 4–8 ms window after the last stimulus (Figure 6B).

### Behavioral Analysis

#### *Wire Hang Test*

To test grip strength, adult mice were placed on a cage top. The cage top was lightly shaken to encourage gripping of the horizontal bars. The cage top was slowly inverted and positioned at least thirty centimeters above the landing surface. The latency to fall was measured. Each mouse underwent this test three times in a single day. With some mice, we repeated the test three times on a separate day. The results did not vary in the additional trials. The average weight of the dI3$^{OFF}$ mice (16.0 ± 3.7 g, n = 5) was not significantly greater than that of the control littermates (16.0 ± 2.6 g, n = 7).

#### *Forepaw Grasp Reflex*

To test for the presence of a forepaw grasp reflex in neonates (P1–P7), we gently stroked the palmar surface of the forepaw with a glass capillary and observed any flexion of the fingers. This test was performed without prior knowledge of the genotype of the pups.

Additional behavioral analyses are described in Supplemental Information.

### Statistical Analysis

Unless otherwise noted, data are reported as mean ± SD, and comparisons were performed using a Student's unpaired t test with unequal variance and a threshold for significance set at 0.05.

## SUPPLEMENTAL INFORMATION

Supplemental Information contains Supplemental Experimental Procedures, five figures, and two movies and can be found with this article online at http://dx.doi.org/10.1016/j.neuron.2013.02.007.

## ACKNOWLEDGMENTS

We thank Angelita Alcos, Bithika Ray, Apiraami Thana, and Nadia Farbstein for excellent technical assistance; Joshua Sanes and Silvia Arber for the generous contribution of mouse strains; Natalie Parks and Dan Marsh for assistance with chronic spinalization; Jason Meissner and Allison Reid for aid with the von Frey test; Anatoliy Voskresenskiy and Leigh Sadler for work with the horizontal ladder experiments; Jonathan Carp and Jonathan Wolpaw for their suggestions in designing the nerve cuff electrodes; Patrick Whelan and Meggie Reardon for help with the isolated spinal cord preparation with sural nerve in continuity; Frédéric Bretzner, Pratip Mitra, Philippe Magown, Izabela Panek, and Sabrina Tazerart for discussions; and Kevin Bourke for photography. We also thank patient D.F., whose disabling grasp reflex led to a portion of the work described. T.V.B. was supported by a Nova Scotia Health Research Foundation fellowship and a Canadian Institutes of Health Research (CIHR) Fellowship. T.M.J. is an investigator of the Howard Hughes Medical Institute and was supported by the National Institutes of Health (R01-NS033245), Project A.L.S., and the Harold and Leila Mathers Foundation. This research was funded by a grant to R.M.B. from the CIHR (FRN 79413) and was undertaken thanks, in part, to funding to R.M.B. from the Canada Research Chairs program.

Accepted: February 1, 2013
Published: April 10, 2013

## REFERENCES

Abdala, V., Manzano, A.S., Tulli, M.J., and Herrel, A. (2009). The tendinous patterns in the palmar surface of the lizard manus: functional consequences for grasping ability. Anat. Rec. (Hoboken) *292*, 842–853.

Akay, T., Acharya, H.J., Fouad, K., and Pearson, K.G. (2006). Behavioral and electromyographic characterization of mice lacking EphA4 receptors. J. Neurophysiol. *96*, 642–651.

Alstermark, B., Pettersson, L.G., Nishimura, Y., Yoshino-Saito, K., Tsuboi, F., Takahashi, M., and Isa, T. (2011). Motor command for precision grip in the macaque monkey can be mediated by spinal interneurons. J. Neurophysiol. *106*, 122–126.

Alvarez, F.J., Villalba, R.M., Zerda, R., and Schneider, S.P. (2004). Vesicular glutamate transporters in the spinal cord, with special reference to sensory primary afferent synapses. J. Comp. Neurol. *472*, 257–280.

Amendola, J., Verrier, B., Roubertoux, P., and Durand, J. (2004). Altered sensorimotor development in a transgenic mouse model of amyotrophic lateral sclerosis. Eur. J. Neurosci. *20*, 2822–2826.

Anderson, K.D. (2004). Targeting recovery: priorities of the spinal cord-injured population. J. Neurotrauma *21*, 1371–1383.

Augurelle, A.S., Smith, A.M., Lejeune, T., and Thonnard, J.L. (2003). Importance of cutaneous feedback in maintaining a secure grip during manipulation of hand-held objects. J. Neurophysiol. *89*, 665–671.

Baker, S.N. (2011). The primate reticulospinal tract, hand function and functional recovery. J. Physiol. *589*, 5603–5612.

Brown, A.G., Fyffe, R.E., Rose, P.K., and Snow, P.J. (1981). Spinal cord collaterals from axons of type II slowly adapting units in the cat. J. Physiol. *316*, 469–480.

Brownstone, R.M., and Bui, T.V. (2010). Spinal interneurons providing input to the final common path during locomotion. Prog. Brain Res. *187*, 81–95.

Brumovsky, P., Watanabe, M., and Hökfelt, T. (2007). Expression of the vesicular glutamate transporters-1 and -2 in adult mouse dorsal root ganglia and spinal cord and their regulation by nerve injury. Neuroscience *147*, 469–490.

Burke, R.E., Degtyarenko, A.M., and Simon, E.S. (2001). Patterns of locomotor drive to motoneurons and last-order interneurons: clues to the structure of the CPG. J. Neurophysiol. *86*, 447–462.

Dimitriou, M., and Edin, B.B. (2008). Discharges in human muscle receptor afferents during block grasping. J. Neurosci. *28*, 12632–12642.

Doyle, M.W., and Andresen, M.C. (2001). Reliability of monosynaptic sensory transmission in brain stem neurons in vitro. J. Neurophysiol. *85*, 2213–2223.

Drew, T., and Rossignol, S. (1987). A kinematic and electromyographic study of cutaneous reflexes evoked from the forelimb of unrestrained walking cats. J. Neurophysiol. *57*, 1160–1184.

Duysens, J., and Pearson, K.G. (1976). The role of cutaneous afferents from the distal hindlimb in the regulation of the step cycle of thalamic cats. Exp. Brain Res. *24*, 245–255.

Egger, M.D., and Wall, P.D. (1971). The plantar cushion reflex circuit: an oligosynaptic cutaneous reflex. J. Physiol. *216*, 483–501.

Ericson, J., Thor, S., Edlund, T., Jessell, T.M., and Yamada, T. (1992). Early stages of motor neuron differentiation revealed by expression of homeobox gene Islet-1. Science *256*, 1555–1560.

Erlanger, J., and Gasser, H.S. (1930). The action potential in fibers of slow conduction in spinal roots and somatic nerves. Am. J. Physiol. *92*, 43–82.

Fetcho, J.R., and McLean, D.L. (2010). Some principles of organization of spinal neurons underlying locomotion in zebrafish and their implications. Ann. N Y Acad. Sci. *1198*, 94–104.

Fetz, E.E., Perlmutter, S.I., Prut, Y., Seki, K., and Votaw, S. (2002). Roles of primate spinal interneurons in preparation and execution of voluntary hand movement. Brain Res. Brain Res. Rev. *40*, 53–65.

Forssberg, H. (1979). Stumbling corrective reaction: a phase-dependent compensatory reaction during locomotion. J. Neurophysiol. *42*, 936–953.

Fox, W.M. (1965). Reflex-ontogeny and behavioural development of the mouse. Anim. Behav. *13*, 234–241.

Fuglevand, A.J. (2011). Mechanical properties and neural control of human hand motor units. J. Physiol. *589*, 5595–5602.

Grillner, S., and Jessell, T.M. (2009). Measured motion: searching for simplicity in spinal locomotor networks. Curr. Opin. Neurobiol. *19*, 572–586.

Gross, M.K., Dottori, M., and Goulding, M. (2002). Lbx1 specifies somatosensory association interneurons in the dorsal spinal cord. Neuron *34*, 535–549.

Grossmann, K.S., Giraudin, A., Britz, O., Zhang, J., and Goulding, M. (2010). Genetic dissection of rhythmic motor networks in mice. Prog. Brain Res. *187*, 19–37.

Haeberle, H., Fujiwara, M., Chuang, J., Medina, M.M., Panditrao, M.V., Bechstedt, S., Howard, J., and Lumpkin, E.A. (2004). Molecular profiling reveals synaptic release machinery in Merkel cells. Proc. Natl. Acad. Sci. USA *101*, 14503–14508.

Halverson, H. (1937). Studies of the grasping responses of early infancy. J. Genet. Psychol. *51*, 371–449.

Helms, A.W., and Johnson, J.E. (2003). Specification of dorsal spinal cord interneurons. Curr. Opin. Neurobiol. *13*, 42–49.

Hnasko, T.S., Chuhma, N., Zhang, H., Goh, G.Y., Sulzer, D., Palmiter, R.D., Rayport, S., and Edwards, R.H. (2010). Vesicular glutamate transport promotes dopamine storage and glutamate corelease in vivo. Neuron *65*, 643–656.

Hongo, T., Kitazawa, S., Ohki, Y., Sasaki, M., and Xi, M.C. (1989a). A physiological and morphological study of premotor interneurones in the cutaneous reflex pathways in cats. Brain Res. *505*, 163–166.

Hongo, T., Kitazawa, S., Ohki, Y., and Xi, M.C. (1989b). Functional identification of last-order interneurones of skin reflex pathways in the cat forelimb segments. Brain Res. *505*, 167–170.

Hooker, D. (1938). The origin of the grasping movement in man. Proc. Am. Philos. Soc. *79*, 587–606.

Jankowska, E. (2008). Spinal interneuronal networks in the cat: elementary components. Brain Res. Brain Res. Rev. *57*, 46–55.

Jennings, E., and Fitzgerald, M. (1998). Postnatal changes in responses of rat dorsal horn cells to afferent stimulation: a fibre-induced sensitization. J. Physiol. *509*, 859–868.

Johansson, R.S., and Flanagan, J.R. (2009). Coding and use of tactile signals from the fingertips in object manipulation tasks. Nat. Rev. Neurosci. *10*, 345–359.

Johansson, R.S., and Westling, G. (1984). Roles of glabrous skin receptors and sensorimotor memory in automatic control of precision grip when lifting rougher or more slippery objects. Exp. Brain Res. *56*, 550–564.

Kiehn, O. (2011). Development and functional organization of spinal locomotor circuits. Curr. Opin. Neurobiol. *21*, 100–109.

Kinoshita, M., Matsui, R., Kato, S., Hasegawa, T., Kasahara, H., Isa, K., Watakabe, A., Yamamori, T., Nishimura, Y., Alstermark, B., et al. (2012). Genetic dissection of the circuit for hand dexterity in primates. Nature *487*, 235–238.

Lagerström, M.C., Rogoz, K., Abrahamsen, B., Persson, E., Reinius, B., Nordenankar, K., Olund, C., Smith, C., Mendez, J.A., Chen, Z.F., et al. (2010). VGLUT2-dependent sensory neurons in the TRPV1 population regulate pain and itch. Neuron *68*, 529–542.

Landry, M., Bouali-Benazzouz, R., El Mestikawy, S., Ravassard, P., and Nagy, F. (2004). Expression of vesicular glutamate transporters in rat lumbar spinal cord, with a note on dorsal root ganglia. J. Comp. Neurol. *468*, 380–394.

Li, W.C., Soffe, S.R., and Roberts, A. (2004). Dorsal spinal interneurons forming a primitive, cutaneous sensory pathway. J. Neurophysiol. *92*, 895–904.

Liem, K.F., Jr., Tremml, G., and Jessell, T.M. (1997). A role for the roof plate and its resident TGFbeta-related proteins in neuronal patterning in the dorsal spinal cord. Cell *91*, 127–138.

Liu, Y., Abdel Samad, O., Zhang, L., Duan, B., Tong, Q., Lopes, C., Ji, R.R., Lowell, B.B., and Ma, Q. (2010). VGLUT2-dependent glutamate release from nociceptors is required to sense pain and suppress itch. Neuron *68*, 543–556.

Lizarraga, I., Chambers, J.P., and Johnson, C.B. (2007). Developmental changes in threshold, conduction velocity, and depressive action of lignocaine on dorsal root potentials from neonatal rats are associated with maturation of myelination. Can. J. Physiol. Pharmacol. *85*, 251–263.

Maricich, S.M., Wellnitz, S.A., Nelson, A.M., Lesniak, D.R., Gerling, G.J., Lumpkin, E.A., and Zoghbi, H.Y. (2009). Merkel cells are essential for light-touch responses. Science *324*, 1580–1582.

Maricich, S.M., Morrison, K.M., Mathes, E.L., and Brewer, B.M. (2012). Rodents rely on Merkel cells for texture discrimination tasks. J. Neurosci. *32*, 3296–3300.

McCrea, D.A. (2001). Spinal circuitry of sensorimotor control of locomotion. J. Physiol. *533*, 41–50.

Mears, S.C., and Frank, E. (1997). Formation of specific monosynaptic connections between muscle spindle afferents and motoneurons in the mouse. J. Neurosci. *17*, 3128–3135.

Mentis, G.Z., Siembab, V.C., Zerda, R., O'Donovan, M.J., and Alvarez, F.J. (2006). Primary afferent synapses on developing and adult Renshaw cells. J. Neurosci. *26*, 13297–13310.

Mestre, T., and Lang, A.E. (2010). The grasp reflex: a symptom in need of treatment. Mov. Disord. *25*, 2479–2485.

Monzée, J., Lamarre, Y., and Smith, A.M. (2003). The effects of digital anesthesia on force control using a precision grip. J. Neurophysiol. *89*, 672–683.

Moschovakis, A.K., Solodkin, M., and Burke, R.E. (1992). Anatomical and physiological study of interneurons in an oligosynaptic cutaneous reflex pathway in the cat hindlimb. Brain Res. *586*, 311–318.

Müller, T., Brohmann, H., Pierani, A., Heppenstall, P.A., Lewin, G.R., Jessell, T.M., and Birchmeier, C. (2002). The homeodomain factor lbx1 distinguishes two major programs of neuronal differentiation in the dorsal spinal cord. Neuron *34*, 551–562.

Napier, J.R. (1956). The prehensile movements of the human hand. J. Bone Joint Surg. Br. *38-B*, 902–913.

Oliveira, A.L., Hydling, F., Olsson, E., Shi, T., Edwards, R.H., Fujiyama, F., Kaneko, T., Hökfelt, T., Cullheim, S., and Meister, B. (2003). Cellular localization of three vesicular glutamate transporter mRNAs and proteins in rat spinal cord and dorsal root ganglia. Synapse *50*, 117–129.

Paulson, G., and Gottlieb, G. (1968). Development reflexes: the reappearance of foetal and neonatal reflexes in aged patients. Brain *91*, 37–52.

Pearson, K.G., Acharya, H., and Fouad, K. (2005). A new electrode configuration for recording electromyographic activity in behaving mice. J. Neurosci. Methods *148*, 36–42.

Pecho-Vrieseling, E., Sigrist, M., Yoshida, Y., Jessell, T.M., and Arber, S. (2009). Specificity of sensory-motor connections encoded by Sema3e-Plxnd1 recognition. Nature *459*, 842–846.

Peyronnard, J.M., and Charron, L. (1982). Motor and sensory neurons of the rat sural nerve: a horseradish peroxidase study. Muscle Nerve *5*, 654–660.

Pietri, T., Eder, O., Blanche, M., Thiery, J.P., and Dufour, S. (2003). The human tissue plasminogen activator-Cre mouse: a new tool for targeting specifically neural crest cells and their derivatives in vivo. Dev. Biol. *259*, 176–187.

Pollack, S.L. (1960). The grasp response in the neonate; its characteristics and interaction with the tonic neck reflex. Arch. Neurol. *3*, 574–581.

Quevedo, J., Stecina, K., Gosgnach, S., and McCrea, D.A. (2005). Stumbling corrective reaction during fictive locomotion in the cat. J. Neurophysiol. *94*, 2045–2052.

Riddle, C.N., and Baker, S.N. (2010). Convergence of pyramidal and medial brain stem descending pathways onto macaque cervical spinal interneurons. J. Neurophysiol. *103*, 2821–2832.

Rogoz, K., Lagerström, M.C., Dufour, S., and Kullander, K. (2012). VGLUT2-dependent glutamatergic transmission in primary afferents is required for intact nociception in both acute and persistent pain modalities. Pain *153*, 1525–1536.

Rushworth, G., and Denny-Brown, D. (1959). The two components of the grasp reflex after ablation of frontal cortex in monkeys. J. Neurol. Neurosurg. Psychiatry *22*, 91–98.

Scherrer, G., Low, S.A., Wang, X., Zhang, J., Yamanaka, H., Urban, R., Solorzano, C., Harper, B., Hnasko, T.S., Edwards, R.H., and Basbaum, A.I. (2010). VGLUT2 expression in primary afferent neurons is essential for normal acute pain and injury-induced heat hypersensitivity. Proc. Natl. Acad. Sci. USA *107*, 22296–22301.

Schieber, M.H. (2011). Dissociating motor cortex from the motor. J. Physiol. *589*, 5613–5624.

Stepien, A.E., Tripodi, M., and Arber, S. (2010). Monosynaptic rabies virus reveals premotor network organization and synaptic specificity of cholinergic partition cells. Neuron *68*, 456–472.

Sürmeli, G., Akay, T., Ippolito, G.C., Tucker, P.W., and Jessell, T.M. (2011). Patterns of spinal sensory-motor connectivity prescribed by a dorsoventral positional template. Cell *147*, 653–665.

Takei, T., and Seki, K. (2010). Spinal interneurons facilitate coactivation of hand muscles during a precision grip task in monkeys. J. Neurosci. *30*, 17041–17050.

Todd, A.J. (2010). Neuronal circuitry for pain processing in the dorsal horn. Nat. Rev. Neurosci. *11*, 823–836.

Todd, A.J., Hughes, D.I., Polgár, E., Nagy, G.G., Mackie, M., Ottersen, O.P., and Maxwell, D.J. (2003). The expression of vesicular glutamate transporters VGLUT1 and VGLUT2 in neurochemically defined axonal populations in the rat spinal cord with emphasis on the dorsal horn. Eur. J. Neurosci. *17*, 13–27.

Tripodi, M., Stepien, A.E., and Arber, S. (2011). Motor antagonism exposed by spatial segregation and timing of neurogenesis. Nature *479*, 61–66.

Vrieseling, E., and Arber, S. (2006). Target-induced transcriptional control of dendritic patterning and connectivity in motor neurons by the ETS gene Pea3. Cell *127*, 1439–1452.

Walshe, F., and Hunt, J. (1936). Further observations upon grasping movements and reflex tonic grasping. Brain *59*, 315–322.

Wang, Z., Li, L., Goulding, M., and Frank, E. (2008). Early postnatal development of reciprocal Ia inhibition in the murine spinal cord. J. Neurophysiol. *100*, 185–196.

Watson, C., Paxinos, G., and Kayalioglu, G. (2008). The Spinal Cord: A Christopher and Dana Reeve Foundation Text and Atlas (London: Acadamic Press).

Witney, A.G., Wing, A., Thonnard, J.L., and Smith, A.M. (2004). The cutaneous contribution to adaptive precision grip. Trends Neurosci. *27*, 637–643.

Young, R.W. (2003). Evolution of the human hand: the role of throwing and clubbing. J. Anat. *202*, 165–174.